Finite element simulation of high-strain dynamic testing of open-toe, steel pipe piles for estimation of geotechnical axial resistance

Juan-Carlos Carvajal [i)] and David Tara [ii)]

i) Senior Geotechnical Engineer, Thurber Engineering, 900 - 1281 West Georgia Street, Vancouver, Canada.

ii) Senior Geotechnical Engineer - Thurber Engineering, 900 - 1281 West Georgia Street, Vancouver, Canada.

ABSTRACT

High-strain dynamic and static loading tests were performed on three open-toe, steel pipe piles driven in a fluvial deposit comprised mainly of compact sand. The pile diameter varied from 0.762 m to 1.524 m and the embedment from 36.5 m to 40 m. Axisymmetric finite element analyses (FEA) were performed with PLAXIS2D to determine the soil properties that control the shaft and the toe resistance of the piles using both dynamic and static load testing data. The geotechnical resistance of the piles obtained with FEA were generally 40% to 70% higher than that obtained with 1D WEA and CAPWAP. The FEA showed that the underestimation of the ultimate pile resistance is at least partially due to the inability to mobilize the toe resistance because of the small peak displacements induced at the pile toe with conventional high-strain dynamic testing (5 mm to 10 mm) in comparison to the large displacements required to mobilize the toe resistance in a static test (65 mm to 140 mm). A procedure is developed to improve the estimation of the ultimate pile resistance for design using FEA and high-strain dynamic load test data.

Keywords: shaft resistance, toe displacement, toe resistance, work time history

1 INTRODUCTION

The geotechnical axial resistance of driven steel pipe piles is commonly obtained with high-strain dynamic testing by measuring the acceleration and the strain in the pile caused by an impact of the driving hammer (ASTM D4945-17). The resistance is determined by matching the measured pile response with that calculated using one-dimensional wave equation analysis (1D WEA), implemented in commercial software.

High-strain dynamic testing is significantly cheaper and faster than static load testing. However, the sensitivity of the matching procedure and the small pile displacement mobilized in the dynamic test can result in underestimation of the geotechnical pile resistance in comparison to that obtained with static load testing, which could impact the foundation cost. In addition, the analyst's experience is a dominant factor in the estimation of the pile resistance with 1D WEA.

This paper describes a simple yet robust procedure for estimating the geotechnical axial resistance of open-toe, driven steel pipe piles using dynamic testing and finite element analysis. The procedure is validated with both static and high-strain dynamic load tests performed on three piles installed in a sand deposit. The pile resistance obtained with the proposed procedure is compared to that obtained with 1D WEA.

2 SITE CONDITIONS

The pile testing site is located on the west coast of British Columbia, Canada. The subsurface conditions consist of a thick succession of deltaic and alluvial sediments (sand, gravel, and silt) up to 130 m depth, overlying a lightly overconsolidated glaciomarine deposit (silt and clay) up to 300 m depth, followed by Glacial till. The ground water table (gwt) is at 2.0 m to 2.8 m depth. The test piles are installed in the deltaic and alluvial sediments to depths of up to 40 m.

The site investigation included cone penetration tests (CPT) and shear wave velocity (V_s) measurements. The interpretation of CPT data up to 50 m depth indicates the soil consists mainly of compact sand interbedded with few lenses of silt and clay. The shear wave velocity increases with depth from about 200 m/s in the upper 5 m up to about 300 m/s at 40 m depth. Figure 1 shows a representative profile of the friction angle and the shear wave velocity obtained from the CPT data. The yellow squares represent the measured V_s.

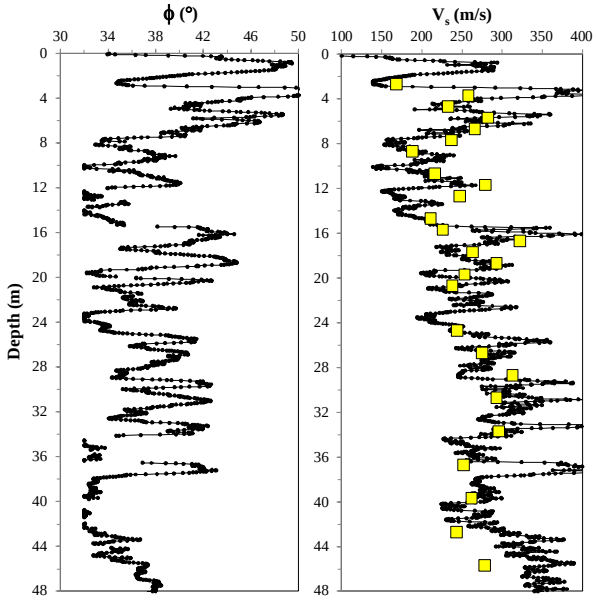

Fig. 1. Representative profiles of peak friction angle (ϕ) and shear wave velocity (V_s) at the pile testing site.

3 FINITE ELEMENT MODEL

The numerical simulation of the static and dynamic pile load tests is carried out with an axisymmetric finite element (FE) model using PLAXIS2D. The components, dimensions, and boundary conditions of the model are shown in Figure 2.

The pile is modeled with an elastic plate element located at x = D/2 from the axisymmetric axis and with embedment L, where D is the pile diameter. The pile projection above ground surface is 500 mm. The input parameters (per meter of perimeter) are the axial stiffness EA (kN/m), the bending stiffness EI (kN·m^2/m), the pile weight w = γ t (kN/m /m), and Poisson's ratio ν = 0.3. In the above parameters, t is the wall thickness, E = 2x10^8 kPa is the Young's modulus of steel, A = t is the unit pile cross-section area, I = t^3/12 is the unit second moment of inertia, and γ = 77 kN/m^3 is the unit weight of steel. Interfaces are added inside and outside of the plate element for modeling the shaft-soil interaction and extended below the pile toe a distance equal to the maximum pile head displacement in the static load test plus 50 mm.

The shear modulus G_{inter} and effective friction angle ϕ_{inter} of the shaft-soil interface (inside and outside) is calculated in PLAXIS2D with the interface strength reduction factor (R_{inter}), which is an input parameter of the adjacent soil material $\rightarrow$ $G_{inter} = (R_{inter})^2 G_{soil}$ and $\phi_{inter} = \tan^{-1}[R_{inter} \tan(\phi_{soil})]$. Gap closure was considered in the interface formulation.

The soil was modeled with the Mohr-Coulomb model, for which input parameters are the soil unit weight γ_{soil} = 19 kN/m^3, Poisson's ratio ν = 0.25, effective cohesion c = 1 kPa (for numerical stability), effective friction angle ϕ, dilation angle ψ = 0°, and the shear wave velocity V_s, which is used as an alternate input parameter for calculating the Young's modulus E_{soil} and the shear modulus G_{soil}. The model was divided into two soil layers for simplicity. Soil 1 represents the soil above the pile toe and controls the shaft resistance. Soil 2 is located below the pile toe with a total thickness of 6D and controls the toe resistance. Soil 2 is extended upward a distance of 6D inside the pile to differentiate the soil properties of the outside shaft resistance from the inside resistance, which is what controls the toe resistance of an open-toe, pipe pile. The 6D dimensions were determined with a sensitivity analysis of simulations of static load tests. The total width of the model is 20 m and the gwt is at ground surface.

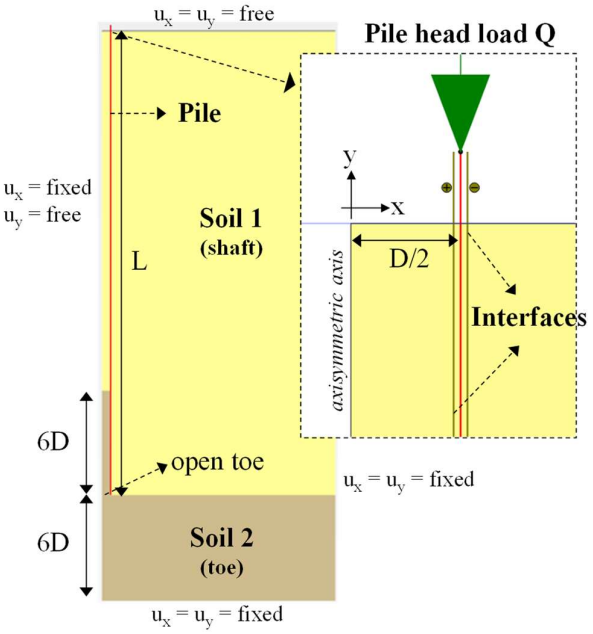

Fig. 2. Axisymmetric finite element model for simulating the static and dynamic axial response of an open-toe, steel pipe pile.

4 SIMULATION OF STATIC LOAD TESTS

The simulation of the static load test is carried out with a displacement-based pushover analysis. The pile head is pushed downwards up to a given target displacement and the unit axial force (kN/m) is extracted from the closest stress point to the pile head. The load-displacement response of the pile head is calculated by multiplying the output unit force with the pile perimeter Per = πD.

The analysis is divided in four phases of plastic analyses: a) initiation of the in-situ stresses using the K_o procedure, b) activation of the plate element (the pile) and the interfaces, c) application of the target displacement $\rightarrow$ loading stage, and d) deactivation of the target displacement $\rightarrow$ unloading stage. The analysis assumes "wished in place" conditions, so no pile installation effects such soil plug development or residual stresses are considered.

The objective of the simulation of the static load test is to determine the properties of the shaft-soil interfaces and the Soil 2 (toe) material that better match the measured load-displacement pile response. Therefore, a calibration procedure is carried out varying the following three input parameters: R_{inter} (same for Soil 1 and Soil 2), and ϕ_{toe} and V_{s_toe} of Soil 2. The properties of the Soil 1 (shaft) material are kept constant ($\phi = 38°$, $V_s = 250$ m/s) since the pile-shaft resistance is controlled by R_{inter}.

The test piles were instrumented only at the pile head and the data consists of load Q and vertical displacement U. The dimensions of the test piles are:

- Pile 1: 762 mm x 16 mm x 36.5 m
- Pile 2: 1067 mm x 19 mm x 35.0 m
- Pile 3: 1524 mm x 25 mm x 40.0 m

Figures 3, 4 and 5 plot the pile head response (Q-U) measured with the static load test and that simulated with the PLAXIS model for Pile 1, Pile 2, and Pile 3, respectively. The pile toe displacement is also plotted for visualization/confirmation of the full mobilization of the shaft resistance (Q_{shaft}) and the mobilization of the toe resistance (Q_{toe}).

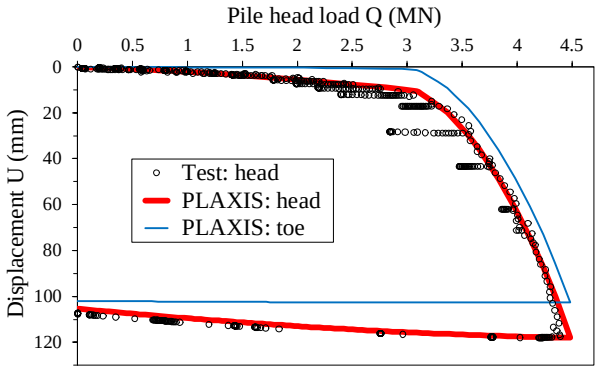

Fig. 3. Simulation of the static load test of Pile 1: ∅762 mm.

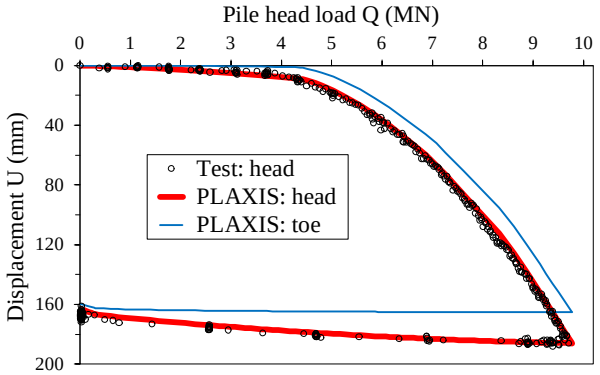

Fig. 4. Simulation of the static load test of Pile 2: ∅1067 mm.

Figures 3 to 5 show that the pile head response simulated with the two-layer, axisymmetric, Mohr-Coulomb, finite element model (PLAXIS) matches very consistently the pile response measured with the static load test for both the loading and the unloading stages.

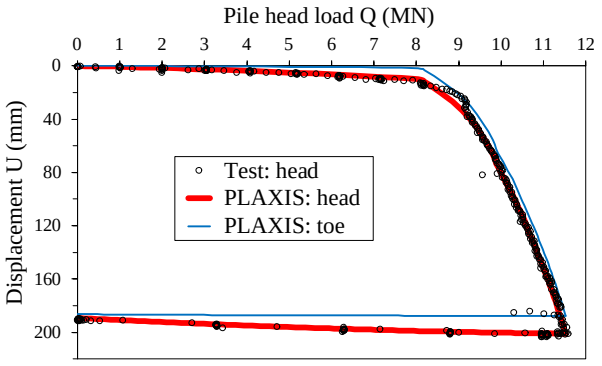

Fig. 5. Simulation of the static load test of Pile 3: ∅1524 mm.

The calibrated soil properties of the FE model are:

- Pile 1: $R_{inter} = 0.47$, $\phi_{toe} = 23.5°$, $V_{s\_toe} = 200$ m/s
- Pile 2: $R_{inter} = 0.51$, $\phi_{toe} = 32.0°$, $V_{s\_toe} = 220$ m/s
- Pile 3: $R_{inter} = 0.53$, $\phi_{toe} = 20.4°$, $V_{s\_toe} = 150$ m/s

The friction angle of the shaft-soil interfaces (obtained from R_{inter}) for Soil 1 (inside and outside the pile) is $\phi_{inter} \approx 20°$ to 23°, and for Soil 2 (inside the pile) is $\phi_{inter} \approx 11°$ to 18°. The shear strength of the interfaces is not only controlled by ϕ_{inter} but also by the vertical and the horizontal stresses, which increase in the Soil 2 interface with the at-rest earth pressure coefficient, $K_o = 1 - \sin(\phi_{toe})$, and the pile toe displacement.

The pile head and pile toe responses in Figures 3 to 5 show clearly the pile head load and displacement for full mobilization of the geotechnical shaft resistance:

- Pile 1: $Q_{shaft} \approx 3.1$ MN, $U_{shaft} \approx 10.3$ mm
- Pile 2: $Q_{shaft} \approx 4.4$ MN, $U_{shaft} \approx 8.9$ mm
- Pile 3: $Q_{shaft} \approx 8.0$ MN, $U_{shaft} \approx 9.6$ mm

For $Q > Q_{shaft}$, the total geotechnical axial resistance ($Q = Q_{shaft} + Q_{toe}$) is controlled by the toe displacement and the associated toe resistance Q_{toe}.

5 LOAD VS DISPLACEMENT EQUATIONS

The static load tests show that the response of the pile head of open-toe, steel pipe piles driven in compact sand is characterized by three loading regions that depend on the pile head displacement: a) the shaft response, b) the toe response, and c) unloading, as shown in Figure 6.

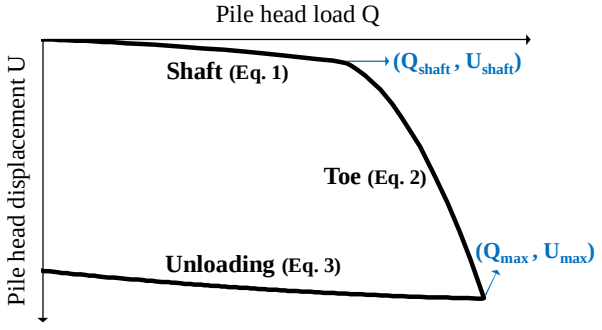

Fig. 6. Loading regions in a static load test of an open-toe, steel pipe pile embedded in compact sand.

Equations 1, 2 and 3 represent proposed formulations (quadratic functions) for calculating the pile head response (Q-U) for the shaft, the toe, and the unloading regions of the static load test, respectively.

$$U = (U_{shaft} - C_{shaft}) [Q/Q_{shaft}] + C_{shaft} [Q/Q_{shaft}]^2 \quad (1)$$

$$U = U_{shaft} + B_{toe} [Q/Q_{shaft} - 1] + C_{toe} [Q/Q_{shaft} - 1]^2 \quad (2)$$

$$U = U_{max} + B_{unload} [Q/Q_{max} - 1] + C_{unload} [Q/Q_{max} - 1]^2 \quad (3)$$

In the above equations, U_{shaft} and Q_{shaft} are the pile head displacement and pile head load that represent the full mobilization of the shaft resistance, and U_{max} is the maximum pile head displacement associated with the maximum pile head load Q_{max} in the static load test, as shown in Figure 6. The remaining parameters C_{shaft}, B_{toe}, C_{toe}, B_{unload}, and C_{unload} control the curvature of the Q-U response. The parameters are determined with an error minimization procedure using either the static load test data or the PLAXIS data of the Q-U pile head response.

The proposed Q-U equations can be implemented in a spreadsheet to facilitate the estimation of the geotechnical pile resistance for a given target pile head displacement or geotechnical resistance factor (ϕ_{gu}).

Figures 7 to 9 plot the Q-U pile head response using Eqs. 1 to 3 (black line), which parameters were obtained using the PLAXIS data (red line) and the function "solver" included in Microsoft Excel.

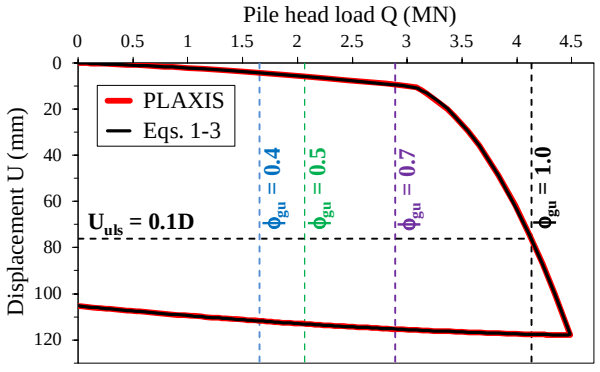

Fig. 7. Curve fitting of the static load test of Pile 1: ∅762 mm

As shown in Figures 7 to 9, the proposed equations match very well the simulation of the static load test with PLAXIS for the loading and unloading regions.

The geotechnical ultimate limit state axial resistance of a pile is associated with a target displacement, which is project dependent and normally taken as U_{uls} = 5% to 15% of the pile diameter D. For this study, the geotechnical ultimate axial resistance (Q_{uls}) is calculated for U_{uls} = 0.1D using the Q-U curves in Figures 7 to 9:

- Pile 1: Q_{uls} = 4.13 MN, U_{uls} ≈ 76 mm
  (Q_{shaft} = 3.06 MN, Q_{toe} = 1.07 MN)
- Pile 2: Q_{uls} = 8.15 MN, U_{uls} ≈ 107 mm
  (Q_{shaft} = 4.39 MN, Q_{toe} = 3.76 MN)
- Pile 3: Q_{uls} ≈ 11.0 MN, U_{uls} ≈ 152 mm
  (Q_{shaft} = 8.01 MN, Q_{toe} = 2.99 MN)

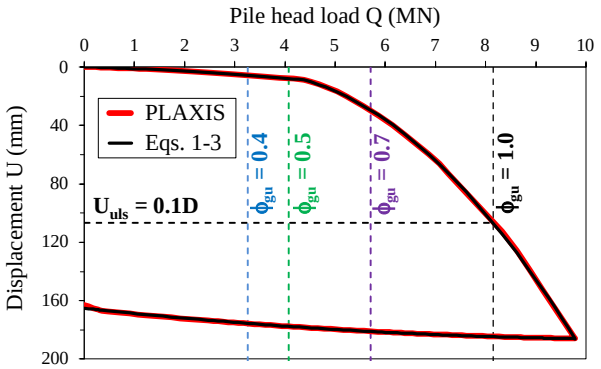

Fig. 8. Curve fitting of the static load test of pile 2: ∅1067 mm.

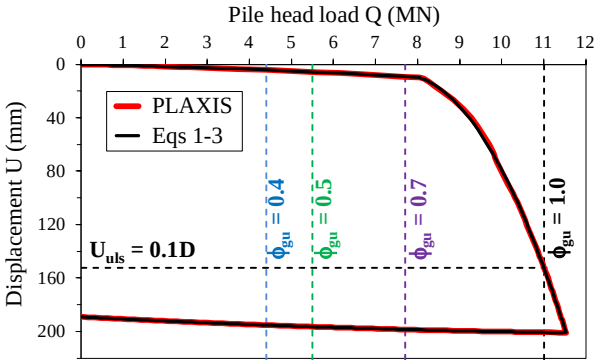

Fig. 9. Curve fitting of the static load test of pile 3: ∅1524 mm.

The geotechnical resistance factor for calculation of the factored axial resistance is ϕ_{gu} = 0.7 if the design is based on a static load test (CSA S6-19). Therefore, the factored resistance ($\Phi Q_{uls} = \phi_{gu} Q_{uls}$) and the associated pile head displacement ($U_{0.7}$) are:

- Pile 1: ΦQ_{uls} ≈ 2.9 MN, $U_{0.7}$ ≈ 9.4 mm (Fig. 7)
- Pile 2: ΦQ_{uls} ≈ 5.7 MN, $U_{0.7}$ ≈ 30 mm (Fig. 8)
- Pile 3: ΦQ_{uls} ≈ 7.7 MN, $U_{0.7}$ ≈ 9.5 mm (Fig. 9)

As shown in Figures 7 and 9, the displacement of the pile head associated with a geotechnical resistance factor ϕ_{gu} = 0.7 is less than 10 mm in Piles 1 and 3, respectively, and it is in the loading region controlled by the shaft resistance. On the other hand, the displacement of Pile 2 is about 30 mm (Fig. 8) and it is in the loading region controlled by the toe response, which is characterized by a steep increase of the pile head displacement (U) with the pile head load (Q).

For a design based on high-strain dynamic testing (ϕ_{gu} = 0.5) or static analysis (ϕ_{gu} = 0.4) with typical degree of understanding of the soil conditions (CSA S6-19), the pile head response is in the loading region controlled by the shaft resistance with associated pile head displacements less than 8 mm, approximately (Fig. 7 to 9.

6 SIMULATION OF DYNAMIC LOAD TESTS

The simulation of the high-strain dynamic load test is carried out with a force-based pushover analysis. The

pile head is pushed downwards with the force time history measured in the dynamic test and the displacement time history is extracted from the closest node to the pile head. The input force for the axisymmetric analysis is calculated as $P_{axi} = P_{test} / 2\pi$, where P_{test} is calculated as the product of E_{steel} and the axial strain time history measured in the dynamic test.

The dynamic analysis is divided in three phases: a) initiation of the in-situ stresses using the K_o procedure, b) activation of the plate element and the interfaces, and c) application of the input force time history. The analysis assumes "wished in place" conditions. The dynamic control parameters are $\alpha = 0.25$, $\beta = 0.5$, and mass matrix = 1.

The objective of the simulation of the high-strain dynamic load test is to determine the properties of the shaft-soil interfaces and the Soil 2 material that better match the total work time history $W_{(t)}$ of the pile head, obtained from the dynamic test data.

$W_{(t)}$ is calculated with the product of the pile head force (P) and the pile head displacement (U) as shown in Equation 4, where the subindexes i and t represent the dynamic time.

$$W_{(t)} = \Sigma \Delta W_i \rightarrow \Delta W_i = \tfrac{1}{2} [P_i + P_{i+1}][U_{i+1} - U_i] \qquad (4)$$

High-strain dynamic analyses are strongly dependent on the viscoelastic damping (energy dissipation) of the pile and the soil. This is modeled in PLAXIS with Rayleigh damping, for which input parameters are two frequencies of vibration (F_1, F_2) and two associated damping ratio values (ξ_1, ξ_2).

Based on sensitivity and parametric analyses carried out for this study, it was determined that the frequencies of vibration for both soil and pile are $F_1 = c/4L$ (the fundamental frequency of vibration of the pile) and $F_2 = 1000$ Hz, where $c = (E_{steel}/\rho_{steel})^{0.5} = 5{,}048$ m/s is the velocity of the axial wave in the pile and L is the sum of the pile embedment and the pile projection. $F_2 = 1000$ Hz makes the dynamic response less dependent on the stiffness and more dependent on the mass of the materials (i.e., pile and soil).

The viscoelastic damping ratio is assumed to be equal for both frequencies ($\xi = \xi_1 = \xi_2$), and for the pile and the soil $\rightarrow$ $\xi = \xi_{soil} = \xi_{pile}$. Therefore, ξ represents the viscoelastic energy dissipation of the entire system: pile + soil + interfaces. Additional energy dissipation is developed in the FE model due to radiation damping and hysteretic damping. The latter is caused mainly by the full mobilization of the shear strength of the shaft-soil interfaces.

The matching of the total work time history of the pile head is carried out between the dynamic times t_o and t_2, where t_o is the initial impact of the hammer and $t_2 = 2L/c$ is the theoretical arrival time of the axial wave in the pile returning from the toe, as shown in Figure 10.

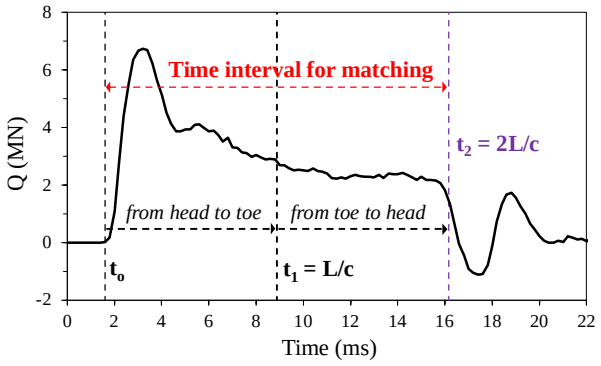

Fig. 10. Force time history measured in the high-strain dynamic test of Pile 1 and selection of the time interval for matching.

The actual time t_2 (arrival of the returning axial wave) is affected by the specific E_{steel}, density ρ_{steel}, L, and pile-soil interaction of the testing pile, and it generally differs from the theoretical $t_2 = 2L/c$ calculated using only L and c = 5,048 m/s. This time difference, however, is small and has a minor effect in matching the total work time history since the variation of the total work (ΔW) tends to be small as t approaches t_2.

The calibration of the FE model is carried out by varying R_{inter} (same for Soil 1 and Soil 2), ϕ_{toe} and V_{s_toe} of Soil 2, and ξ (same for the pile, Soil 1, and Soil 2). The properties of Soil 1 are kept constant ($\phi = 38°$, $V_s = 250$ m/s).

6.1 Matched total work time history

Figures 11, 12, and 13 plot the total work time histories obtained from the high-strain dynamic test and from the calibrated PLAXIS model for Pile 1, Pile 2, and Pile 3, respectively. EOD and BOR stand for end of initial driving and beginning of restrike, respectively.

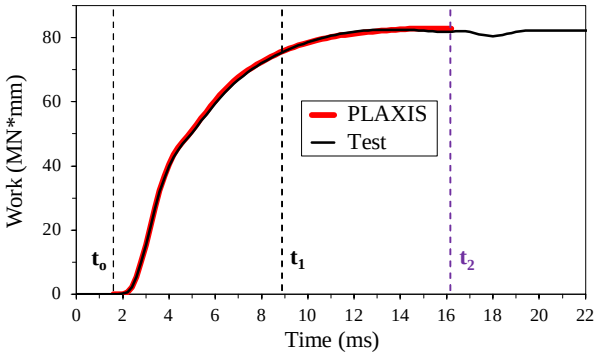

Fig. 11. Total work time history of Pile 1-EOD: ∅762 mm.

As shown in Figures 11 to 13, the match of the work time histories between the dynamic test and the PLAXIS model in the time interval of interest (t_o - t_2) is very good.

The calibrated properties of the PLAXIS model are:

- Pile 1 - EOD: $R_{inter} = 0.22$, $\xi = 12\%$
- Pile 2 - BOR: $R_{inter} = 0.51$, $\xi = 15\%$
- Pile 3 - EOD: $R_{inter} = 0.34$, $\xi = 20\%$

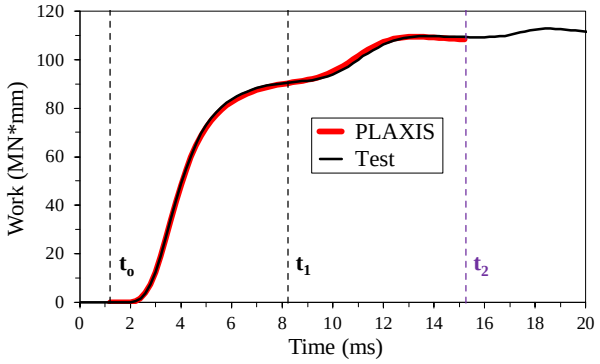

Fig. 12. Total work time history of Pile 2-BOR: ∅1067 mm.

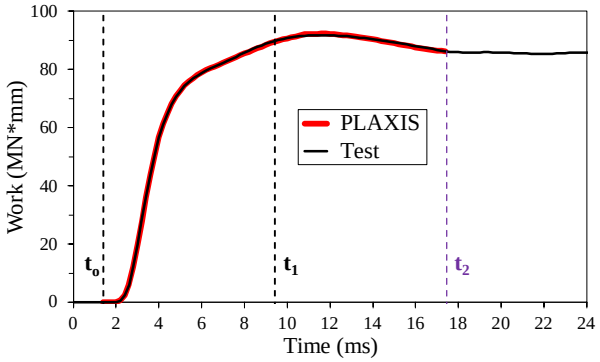

Fig. 13. Total work time history of Pile 3-EOD: ∅1524 mm.

The calibration of the FE model indicated that the dynamic response of the pile is practically insensitive to the properties of the Soil 2 material (ϕ_{toe}, V_{s_toe}) for the three tested piles. This may be due to the very small displacement induced at the pile toe during the dynamic test (< 5 mm) as shown in Figure 14 with the blue line.

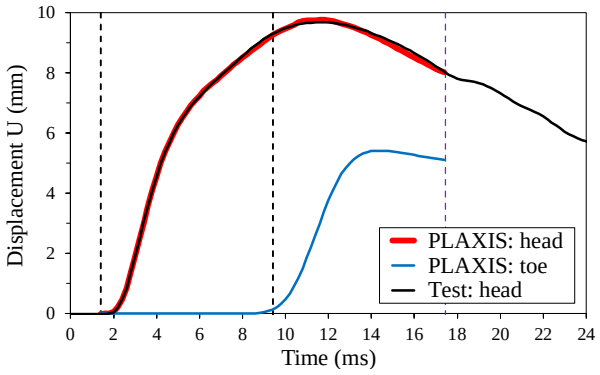

Fig. 14. Displacement time history of Pile 3-EOD: ∅1524 mm.

Therefore, it is concluded that the pile resistance obtained from the simulation of the high-strain dynamic test represents mainly the shaft resistance due to the small displacement of the pile head and the pile toe mobilized during the test. Because of the limitation of the mobilized pile displacement in the dynamic test, the soil properties of the toe material (ϕ_{toe}, V_{s_toe}) cannot be accurately determined for the three tested open-toe piles, embedded in compact sand.

6.2 Pile head force vs displacement

Figures 15, 16, and 17 plot the force vs displacement response of the pile head during the dynamic test for Pile 1, Pile 2, and Pile 3, respectively, for the time interval of interest (t_o-t_2). As shown in the figures, the simulation of the high-strain dynamic test with the PLAXIS model agrees reasonably well with the measured test data, especially for test Pile 3.

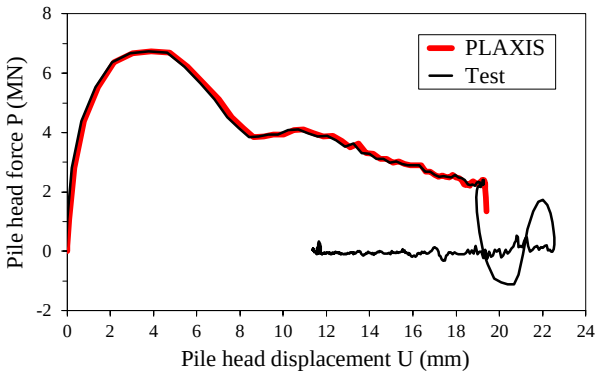

Fig. 15. Force-Displacement response of Pile 1-EOD: ∅762 mm.

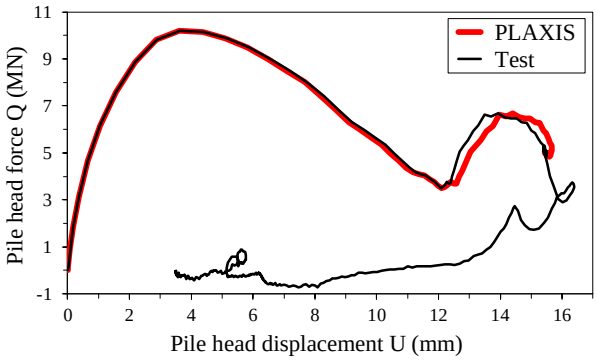

Fig. 16. Force-Displacement response of Pile 2-BOR: ∅1067 mm.

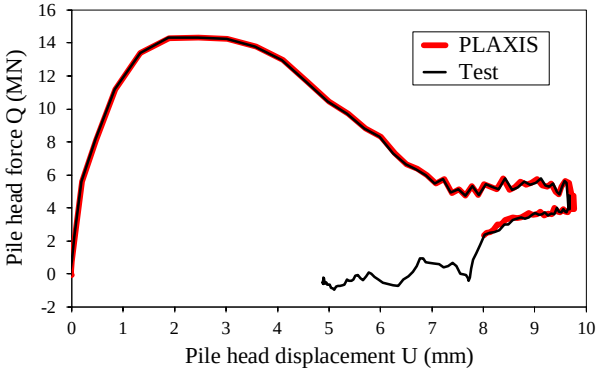

Fig. 17. Force-Displacement response of Pile 3-EOD: ∅1524 mm.

6.3 Geotechnical ultimate axial resistance

The estimation of the geotechnical resistance of the pile is carried out by simulating a static test (Q-U) using the strength reduction factor of the interfaces (R_{inter})

calibrated with the high-strain dynamic test data. Since the properties of the Soil 2 material (toe) could not be determined with the dynamic test data, the simulation of the static test is performed using the toe soil properties obtained with the calibration of the static load test data.

Figures 18, 19 and 20 plot the pile head response (Q-U) simulated with a static load test for Pile 1, Pile 2, and Pile 3, respectively.

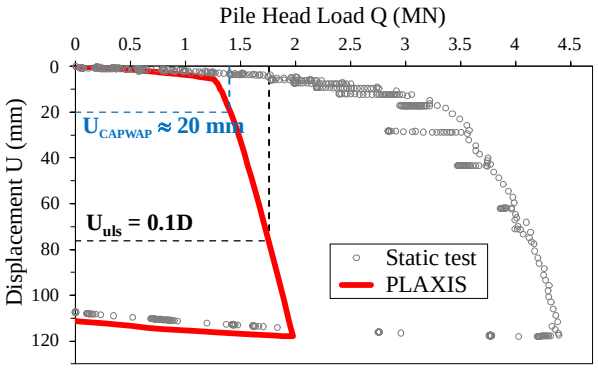

Fig. 18. Simulation of a static load test for Pile 1: EOD.

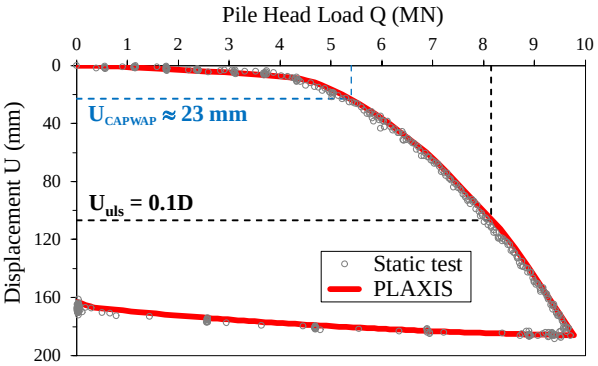

Fig. 19. Simulation of a static load test for Pile 2: BOR.

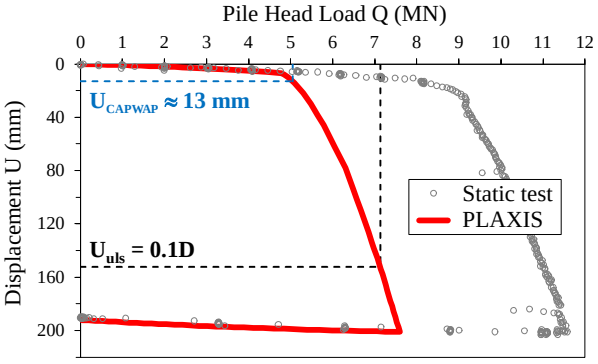

Fig. 20. Simulation of a static load test for Pile 3: EOD.

The interface strength reduction factor for Pile 2 calibrated with the high-strain dynamic load test data for BOR is the same as that calibrated with the static load test data → R_{inter} = 0.51. Therefore, the simulated static load test in Pile 2 using the dynamic test data matches the static load test very well (Fig. 19).

The geotechnical ultimate axial resistance is obtained from the Q-U pile head response (PLAXIS) for U_{uls} = 0.1D. Figures 18 to 20 also indicate the peak pile head displacement obtained from the dynamic test using 1D WEA and CAPWAP (U_{CAPWAP}) and the associated pile head load using the Q-U PLAXIS response. These displacements are slightly higher than the peak displacements of the dynamic test because of the methodology in CAPWAP for estimating the geotechnical resistance.

Figure 21 shows the estimation of the geotechnical axial resistance of the piles using CAPWAP, PLAXIS for U = U_{CAPWAP}, and PLAXIS for U_{uls} = 0.1D.

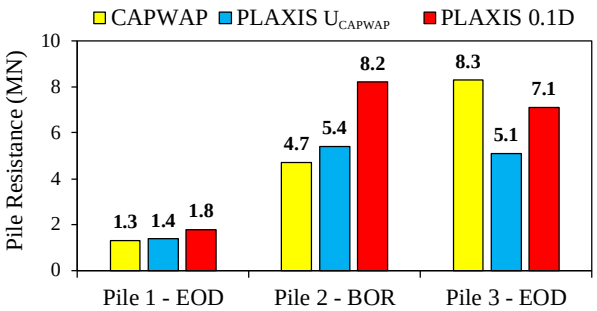

Fig. 21. Geotechnical pile resistance obtained using the high-strain dynamic load test data.

Figure 21 shows that the estimation of the pile resistance with PLAXIS for U = U_{CAPWAP} is about 8% to 15% higher than that estimated with CAPWAP. This is considered a small difference for practical purposes. On the other hand, the resistance obtained with PLAXIS (U_{CAPWAP}) for Pile 3 is about 39% lower than that estimated with CAPWAP. The estimation of the resistance with CAPWAP for Pile 3 seems too high since it was obtained at the end of driving with just 13 mm of pile head displacement during the dynamic test, yet it is just 25% lower than the resistance obtained with the static load test, which accounts for soil setup, → 8.3 MN (EOD) vs 11.0 MN (static test). On the other hand, the resistance obtained with the PLAXIS model for the same pile head displacement (13 mm) is about 54% lower than that of the static load test: 5.1 MN vs 11 MN, which seems consistent for the expected EOD resistance.

Note that the estimation of the geotechnical resistance with CAPWAP depends strongly on the experience of the analyst. Therefore, the overestimation of the EOD resistance of Pile 3 may be the result of that.

For a pile head displacement U = 0.1D, Figure 21 shows that the geotechnical resistance obtained with the PLAXIS model increases and is about 38% and 74% higher than that estimated with CAPWAP for Pile 1 and Pile 2, respectively. The main reason for the increase in the resistance is the increase in the pile head displacement and the ability to mobilize higher toe resistance. On the other hand, the resistance obtained with the PLAXIS model (U = 0.1D) for Pile 3 is about

14% lower than that estimated with CAPWAP.

7 CONCLUSIONS

This study reviewed the development of a procedure for estimating the axial resistance of open-toe, steel pipe piles driven in compact sand using high-strain dynamic load testing.

The procedure is based on matching the total work time history of the pile head obtained with the high-strain dynamic load test with that obtained using an axisymmetric finite element model. The matching procedure requires calibration of the shaft resistance and the damping of the dynamic system.

The calibration of the finite element model indicated that the dynamic response of the pile head is practically insensitive to the properties of the soil material that controls the toe resistance (ϕ_{toe}, V_{s_toe}). This seems to be due to the very small displacements induced in the pile toe during the high-strain dynamic test (< 5 mm).

The estimation of the geotechnical resistance of the pile is carried out by simulating a static load test (Q-U) using the strength reduction factor of the interfaces (R_{inter}) calibrated with the high-strain dynamic test data. Since the properties of the soil material that control the toe resistance could not be determined with the dynamic test data, the simulation of the static test is performed using the toe soil properties obtained with the calibration of the finite element model using the static load test data. In the absence of a static load test, the properties of the toe soil material can be assumed using the site investigation data.

The geotechnical resistance obtained with the proposed procedure and finite element model for test Pile 1 and Pile 2 is 38% and 74% higher, respectively, than that obtained with CAPWAP. This is the result of the higher pile head displacement mobilized with the simulated static load tests (PLAXIS: 76 mm to 152 mm) in comparison to that mobilized in the high-strain dynamic load test (13 mm to 23 mm).

REFERENCES

1) ASTM International (2017): Standard Test Method for High-Strain Dynamic Testing of Deep Foundations. ASTM D4945-17.

2) CAPWAP: Case Pile Wave Analysis Program. PDI - Pile Dynamics, Inc.

3) CSA S6-19: Canadian Highway Bridge Design Code.